Journal of Medicinal and Chemical Sciences 5 (2022) 1331-1346

Journal of Medicinal and Chemical Sciences

Journal homepage: http://www.jmchemsci.com/

Original Article (Special Issue)

Microwave Synthesis Schiff Base from Drug and 1,10-Phenanthroline/8-Hydroxyquinoline as a Co-ligand with Complexes: Cytotoxic, Antimicrobial, and DNA Interaction Efficacy

Hiyam Hadi Alkam*, Rehab K. Al-Shemary

Department of Chemistry, College of Abn-Alhitham, Baghdad University, Iraq

ARTICLE INFO

Article history

Receive: 2022-06-20
Received in revised: 2022-07-29
Accepted: 2022-09-01
Manuscript ID: JMCS-2207-1590
Checked for Plagiarism: **Yes**
Language Editor:
Dr. Behrouz Jamalvandi
Editor who approved publication:
Professor Dr. Ali Delpisheh

DOI:10.26655/JMCHEMSCI.2022.7.22

KEYWORDS

Schiff base
Benzophenone
Octahedral geometry
Antimicrobial

ABSTRACT

Trimethoprim and benzophenone are mixed to form the Schiff-base of the N_2O donor ligand. Various spectroscopies are used to describe the ligand. Numerous new mixed ligand complexes of two ligands are produced with Ni(II), Co(II), and Cu(II) ions, where Schiff base = (L_1) (1,10-Phen) and deprotonated (8-HQ = (L_2).(MO)metal oxide is the last product of heat breakdown for specific complexes, according to research. Additionally, water molecules that are linked to complexes are found to be coordinated or crystalline by thermal gravimetric measurement (TGA). The Schiff base preparation technique yields complexes of Co(II), Ni(II) and Cu(II) with octahedral geometry (for 1,10-PhenIn addition, antimicrobialmixed ligand complexes have been tested against the pathogenic strains of bacteria and fungus types, whichare*Escherichia Coli*, *Bacillus subtilis* ,*Eterobacter*and*Staphylococcus aureus*,F.solani and C.cucurbitacin.A549, HaCaT and MCF-7 anticancer cell lines have been investigated. The outstanding result of mixed Cu(II) complexes was highlighted.

GRAPHICAL ABSTRACT

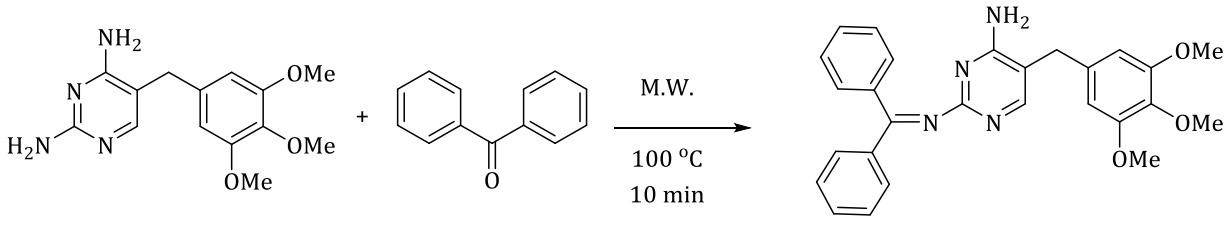

* Corresponding author: Hiyam Hadi Alkam
✉ E-mail: heam.h.a@ihcoedu.uobaghdad.edu.iq

Introduction

Schiff bases are azomethine-containing compounds (-C=N-) formed by the condensation reaction of primary amines and carbonyl compounds containing aldehydes or ketones [1]. Severalprocesses have been utilized for Schiff base preparation [2]. Greener procedures of preparation Schiff bases have also been noticed. However, all of these methodologies have some drawbacks such as drying agent cost [3], long reaction time [4], special devices [5], special situations, *etc*. [6]. The reactions were extensively investigated with the help of a microwave, as mentioned in the initial research [7]. Another distinguishing feature is that they form stable complexes with the majority of transition metal ions, making them an important ligand family in coordination chemistry. Microwave methods have been commonly utilized to prepare Schiff base by synthesizing organic [8]. Furthermore, they have a wide range of applications in biological [9], clinical [10], medicinal [11], electrochemistry [12], analytical [13], and industrial [14] research, as well as being used as medicinal [15], liquid crystals [16] in analytical, and polymer chemistry [17].Chemists of organic are attentive to prepare Schiff bases attributed to such considerable activities of biological [18]. Cancer [19], metal-mediated antibiotics [20], antiviral [21], radio sensitizers [22], antibacterial [23], and antiparasitic research are all underway [24]. They form metal chelate complexes with a number of biologically significant bivalent ions [25]. Here, we describe the synthesis of the Schiff base from benzophenone and trimethoprim coupled with 1,10-phenanthroline/8-hydroxyquinoline, as well as its characterization. This Schiff base is made of the metal complexes Ni(II), Co(II), and Cu(II). It was also mentioned that some bioactivity test results showed that ligands and their metal complexes had antibacterial, DNA interaction effectiveness and antioxidant characteristics.

Materials and Methods

Appliances and reagents: All reagents trimethoprim, benzophenone acid 1,10-phenanthroline/8-hydroxyquinoline and various metal (II) chlorides were of Merck produces and utilized as provided. Anhydrous grade methanol and DMSO were cleared according to normal procedures. Micro-analytical datum, ^{1}H and ^{13}C NMR spectra of the components were recorded Bruker specrospin ultra shield magnets 300 MHz instrument. The IR spectra of the samples were recorded on a Shimadzu FTIR–8400 Fourier Transform Infrared Spectrophotometer in 4000∼200 cm^{-1} range utilizing KBr pellet. The UV-Vis. spectra were recorded on a Shimadzu. Finally, the biological activity against various microorganisms has performed the complexes and ligand. Molar conductivity of the complexes was measured on pw 9526 digital conductivity in DMSO at 10^{-3}M. Magnetic susceptibility was recorded by magnetic susceptibility balance, made, Ms-BMKI and made in Al-Nahrain University.

Synthesis of ligand

Trimethoprim (0.05 mmol) is mixed with benzophenone (0.05 mmol) in a 1:1 proportion molar and the solution is ground in a ceramic mortar. In addition, for 10 minutes, the ingredients are exposed to microwave radiation at (100 da C). Finally, a small fraction of dry benzene cleaned the output (Scheme 1).

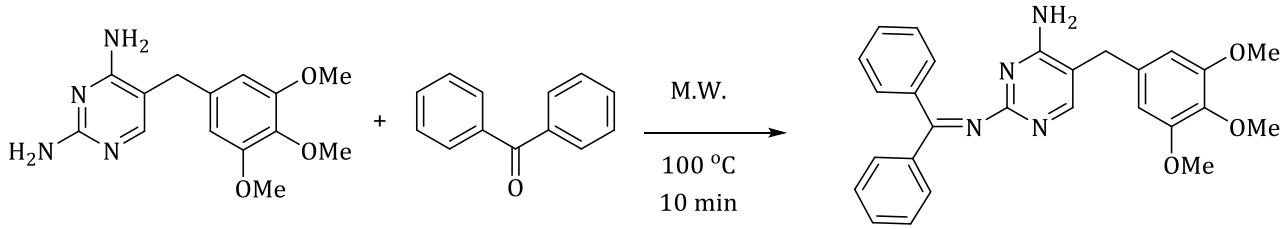

Scheme 1: The Schiff base preparation course

Synthesis of complexes

Complexes were produced by refluxing a (25 mL) ethanol solution of a Schiff base and metal (II) chloride for two hours with four drops of KOH solution. The precipitated solids [Co(II), Ni(II), and Cu(II)] were filtered with suction, washed with ethanol, and dried on the silica gel (Scheme 2).

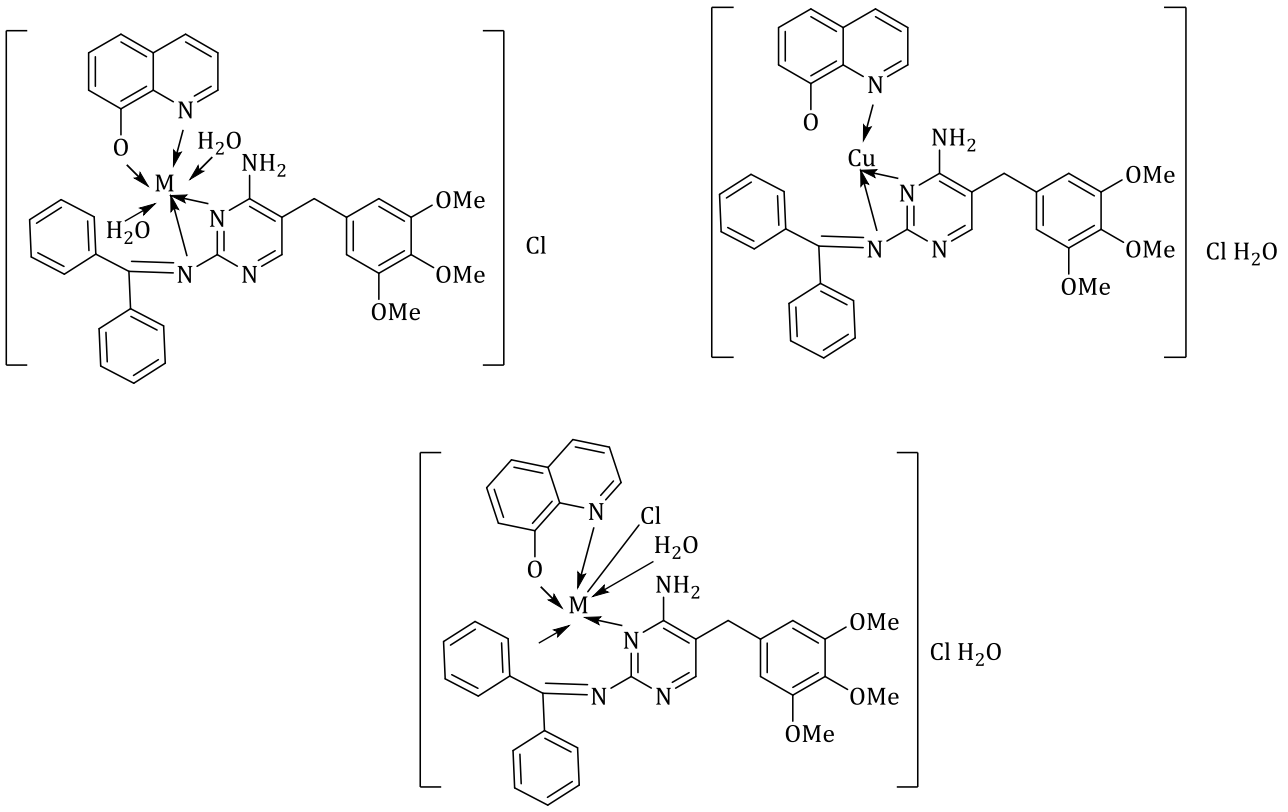

Scheme 2: Proposed structure for the mixed ligand complexes

Evaluation of the biological activity of the compounds

Fusarium solani served as the experiment's screen fungus. From each mixed complex, 1mL of *Cercosporacucurbitacin* solution (0.01 g/mL) was made. PDA (sterile molten potato dextrose agar) in the amount of 15 ml was aseptically allowed to solidify at room temperature and combined with it before being poured onto plates. They used to control as benlate. Using a sterile 4mm cork borer, they were injected in the middle of the plates. The evolution of the antifungal strains included *Fusarium solani* and *Cercosporacucurbitacin* was tested at 24 hours while all plates were cultured incubated hrs at 27 °C for 48.

Moreover, the bacteria utilized for this experience contained *Pseudomonas*, *aeruginosa*, *Escherichia Coli, Bacillus subtilis, Eterobactern and Staphylococcus aureus*. They were incubated at 37 °C for 18-24 hrs and were seeded on (NA) plates containing 8mm wells. An of each complexe**s** concentration.

Cytotoxicity studies

Cell culture and treatment

We employed the HaCaT normal human keratinocytes, L132 human lung embryonic cells, A549 and MCF7 human cancer cell lines. They were grown in NUNC T-cell flasks with (100 units/mL) penicillin, (100 g/mL) streptomycin, (5% CO_2 and 95% O_2) (2.5 g/ml) amphotericin B, and (100 g/mL) gentamicin. They were subcultured and employed for experiments once they had been trypsinized to a confluence of between 70 and 80%. Using the MTT test, the cytotoxicity of substances on cancerous and

healthy cell lines was evaluated. In this test, cell viability was evaluated by transforming yellow fluorescent protein, a technique created by Mabley et al. The complexes were added to the cells after they had been plated on 96 healthy plates at a density of 4X104/well using DMEM culture medium. The complexes were then treated at varied concentrations starting at 2 µM, 5 µM, and 10 µM. The MTT assay has been performed in triplicates. Following a 24 hr period of incubation, cells have been studied with a phase-contrast microscope to determine their morphology and were then captured on camera by Leica systems. The medium has been then taken out. The cells have been then cultured for 4 hrs in CO_2 incubator with 0.5 mg/mL of MTT. After four incubations with the MTT solution, the solution has been discarded, and 200 L of DMSO was used to dissolve the blue formazan crystal. Using a BioRad ELISA plate reader, the absorbance was calculated at 570 nm.

Cellular morphology assessment. (AO)/ (PI) dual staining

HaCaT and A549 cells were plated at 5104 density in 6-well plates. They were raised to grow until they were 80–70% confluent at 37 °C in an incubator with dampened CO_2. Additionally, they received 24-hour treatment with a range of complicated dosages (2, 1, and 0.5 M). The culture was gently douched from each cell and then washed twice in PBS at 25 °C. Staining was done on the egalitarian cell counts from the metallic moiety and the control.

Table 1: some physical characteristics and micro-analysis of all of the products that have been prepared

Compounds	Empirical Formulae	(Formula wt.)	Yield %	Color	Elemental Analysis Found (Calc.) %(estimated)				
					C	H	N	M	Cl
[L]	$C_{27}H_{26}N_4O_3$	454.53	77	Off white	70.87 (71.35)	5.31 (5.77)	12.01 (12.33)	-	-
$[Co(L)(Q)(H_2O)_2]Cl.H_2O$	$C_{36}H_{36}CoN_5O_6Cl$	729.10	82	brown	59.06 (59.31)	4.21 (4.98)	8.89 (9.61)	7.76 (8.08)	4.35 (4.86)
$[Ni(L)(Q)H_2O)_2]Cl.H_2O$	$C_{36}H_{36}NiN_5O_6Cl$	728.86	78	green	59.244 (59.33)	4.58 (4.98)	9.49 (9.61)	7.88 (8.05)	4.45 (4.86)
$[Cu(L)(Q)]Cl.H_2O$	$C_{36}H_{34}CuN_5O_5Cl$	714.64	67	Reddish -brown	59.76 (60.42)	4.37 (4.79)	9.22 (9.79)	8.12 (8.88)	4.76 (4.95)
$[Co(L)(PHH))(H_2O)_2Cl]Cl.H_2O$	$C_{35}H_{32}CoN_6O_3Cl$	679.06	82	Olive	61.23 (61.91)	12.08 (12.38)	8.52 (8.86)	8.52 (8.86)	5.32 (5.22)
$[Ni(L)(PHH))(H_2O)_2Cl]Cl.H_2O$	$C_{36}H_{32}NiN_6O_3Cl$	678. 82	78	Pale green	61.21 (61.91)	4.62 (4.75)	11.55 (12.38)	8.11 (8.65)	
$[Cu(L)(PHH)(H_2O)_2Cl]Cl.H_2O$	$C_{36}H_{32}CuN_5O_4Cl$	683.68	67	Green	61.32 (61.49)	4.12 (4.72)	9.38 (10.04)	8.76 (9.29)	4.85 (5.19)

Results and Discussion

The specific bands of IR spectra of prepared compounds are summered in Table 3. The IR

spectra of complexes appear bands around 3276–3486cm^{-1} assigned to (OH) molecules of H_2O related to the complexes [18]. From 1627–1659 cm^{-1}, complexes' (C=N) band is shifted towards lower wavenumbers than the free ligand band at 1676cm^{-1}[9]. This change shows that the two groups of (C=N) have coordinated with the metal ions. The presence of a (C–O) band at substantially lower frequency values 1210–1220 cm^{-1} than ligand 1236 cm^{-1} shows that the Schiff-hydroxyl base's groups coordinate with metal ions. In the Schiff base spectra, the two peaks at found at 3421-3421 cm^{-1} and 3377-3421 cm^{-1} that have been assigned to stretching of υ $_{sym}$ and $_{asy}$ (NH_2) [10]. No change in frequencies indicated no coordinations of the metal ions through N atoms of NH_2 groups in complexes. Bands have been observed at 1576 cm^{-1}, and 1572 cm^{-1} which have been a result of the C=N imine groups in the rings for [Phen], and [8HQ] ligands, respectively. whereas those bands have been shifted to lower frequency values ranging within (l560-1550) cm^{-1} and l526 -l496 cm^{-1}as a result of reduction of the υ C=N bond of imine group and indicates that band of the ligands (8-HQ and Schiff base) coordinate to metal ions through *N*-azomethine groups in rings. New bands in 524–610 cm^{-1} and 454–498 cm^{-1} ranges have been tentatively ascribed to (M–O) and (M–N), respectively. Indicating that the O-phenolic atoms and N-atoms of C=N [11]. Additionally, the latter complexes lacked broad stretching vibration at 3253 cm^{-1} caused by the (O-H) group of 8-HQ ligand, indicating that an M-O bond had been formed with 8-HQ. Which is why, the 8-HQ functions as a bidentate chelating ligand in all of the compounds [12].

Table 2: All of the produced compounds' FT-IR spectral data (cm^{-1})

Compound	ν (M-O)	ν (M-N)	ν (C-O)	δ(H_2O)	ν(C=N)imine	ν(C=N)$_{Pyr.}$ ν(C=N)$_{Q}$	ν(N-H)$_{asym}$	ν(N-H)$_{sym}$	υ(OH.)$_{Q}$	ν (M-O)
[L]	-		-	-	1667	1576 -		3421 3377	3253	-
[8HQ]	-	-	1236	-	-	- 1572			3182	-
PPH	-	-	-	-	-	1566				-
[Co(L)(Q)(H_2O)$_2$]Cl.H_2O	498	603	122	603	1639	*l562* *l526*	3468 3391		*3276*	498
[Ni(L)(Q) H_2O)$_2$]Cl.H_2O	481		1236	578	1640	1563 1512	3455 3389		*3486*	481
[Cu(L)(Q)]Cl.H_2O	454	578	1236	610	1636	1560 1508	3468 3396		-	454
[Co(L)(PHH))(H_2O)$_2$Cl]Cl. H_2O	465			564	1638	1558 1496	3460 3398		*3265*	465
[Ni(L)(PHH))(H_2O)$_2$Cl]Cl. H_2O	472	610		572	1636	1553 1419	3468 3386		*3258*	472
[Cu(L)(PHH) (H_2O)$_2$Cl]Cl. H_2O	488			585	1634	1550 1498	3452 3364		*3282*	488

NMR Spectra

The ^{1}H-NMR spectra of the ligand [L] in DMSO-d_6 was seen. The signal is visible in [L1H-NMR]'s spectra as a singlet at 3.67, 3.72, and 3.80 ppm for the protons of the (OCH_3) group (9H). The ($-CH_2$) group proton at 3.67 ppm is what's causing the singlet signal (2H). Proton signal of the (NH_2) group at 6.84 ppm (2H). The atomic protons are numerous at 6.48 to 8.34 ppm (13H). At 2.49 ppm [12], figure, the DMSO signal had begun to appear (1). The ligand's 13C NMR spectrum revealed peaks at (176.7) ppm and 162.3 ppm, which correspond to the C=N and ($=C-NH_2$) groups, respectively. The chemical changes caused by two (C=N) groups in a ring were at 158.8 ppm and 159.6 ppm, respectively. The range of (103.43-134.2) ppm has been used to attach signals to (C=C) aromatic carbon. At 35.3 ppm, (CH_2) chemicalshifting was seen. The three chemical shifts at ppm (58.4), (59.8), and (61.8).

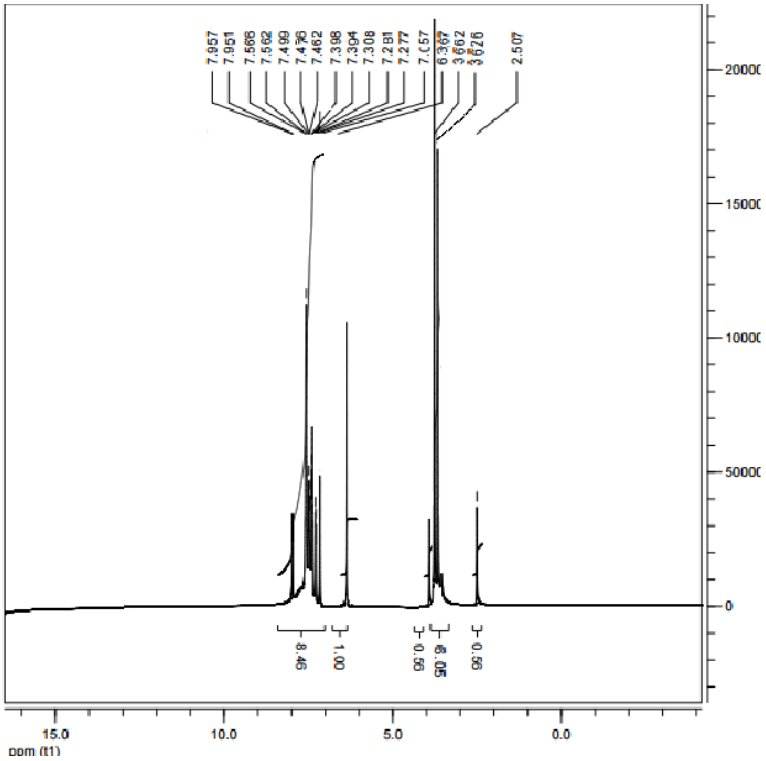

Figure 1:^{1} H NMR spectra of ligand [L]

UV-Vis Spectroscopic, magnetic moment studies ligands spectra appeared two absorption bands in the 200–220 nm and 231–237 nm. The former band is for the absorption of (n– π*) transmission of the C=N moiety after chelation. The last broad peak is designated to inter-molecular CT and n– π * transmission from ligand to metal ions [14]. Complexes spectra had exhibited various absorption peaks, containing absorption peaks of the ligands and d–d transmissions of metal ions. Spectra of complexes, the 1st band of ligands (200–220nm), are autonomous of complexation. The 2nd peak for complexes places in region of (274–286nm). The 3rd peak is ascribed to π→ π* transmissions participating C=N found at 345–365nm. The peak at 390–430nm is designated to CT transmissions. The spectra of the [Co(L)(PPH)$(H_2O)_2$Cl] and[Co(L)(Q)$(H_2O)_2$]Cl.H_2O complexes appear 2 d–d transmissions peaks in 515nm –650nm. The two peaks are designated to $^4T_1g \rightarrow {}^4T_1g_{(P)}$ and $^4T_1g \rightarrow {}^4T_1g_{(F)}$ transmissions of the octahedral system [15]. The β data are lower than unity suggesting strong bonds of M–L covalent. Depended on 10Dq data, the base kind has a large impact on transmission energy. The arrangement is empirically proposed to be as follows: 1,10-Phen>8-HQ[16]. The molar conductance data for [Co(L)(Q)$(H_2O)_2$]Cl, [Ni(L)(Q)(H2O)2]Cl.H_2O, and [Cu(L)(Q)]Cl.H_2O in DMF solution (10^{-3} M). DMF shifting the chelated

chloride ions indicates that these complexes are 1:1 electrolytes. Further, the molar conductance data of $[Co(L)(Q)(H_2O)_2]Cl.\ H_2O$, $[Ni(L)(PPH)Cl]$, and $[Cu(L)(PPH)Cl]$ proposes the non-electrolytic nature of the complex. The $[Ni(L)(Q)(H_2O)_2]Cl.H_2O$complex spectrum appears band at 470nm is designated to $^3A_2g \rightarrow {}^3T_1g_{(P)}$ transition in $[Ni(L)(PPH)(H_2O)_2]Cl$ complex at same region. The latter transmission is a less peak around640nm, attributed to the existence of the octahedral system. It is ascribed to the $^3A_2g \rightarrow {}^3T_2g$ transmission [17]. These complexes' B and 10Dq data have been determined, and 10Dq data suggest which bases follow arrangement: 8-HQ> 1,10-Phen..The total magnetic moments for Ni(II) complexes are in arange of (4.61–4.86) BM. and for the Cu(II) complexes are in the reign (1.78–1.81) BM. while for the Co (II) complexes are in the reign (4.72-4.87) BM. In (10^{-3} M) of DMSO complexes have molar conductances of (33.21 -75.1) $Ohm^{-1}\ cm^2\ mol^{-1}$, with all complexes being 1:1 electrolytes.The magnetic moments and UV spectra of complexes can determine whether the metal ions have an octahedral structure excepted $[Cu(L)(Q)(H_2O)]Cl$ [18].

Table 3: UV-Vis magnetic andspectralmoment values (nm) of compounds in the DMSO

Compounds	Λmohm .cm^2 $molar^{-1}$	λ nm	$\upsilon_{cm^{-1}}$	ε_{max} ($molar^{-1}.cm^{-1}$)	Transitions	μe_{ff} (BM)	geometry
[L]		217 235	46,08242,553	2045 2354	π→π* n→π*	-	-
8HQ		220 231	45,45443,290	834 1821	π→π* n→π*	-	-
PPH		210 237	47,61942,194	1123 1871	π→π* n→π*	-	-
$[Co(L)(Q)(H_2O)_2]Cl.H_2O$	60.67	218 274 356 430 698 787	45,871 36,231 28,089 14,326 12,706	2478 1831 1427 58 30	L.F L.FC.T$^4T_1g \rightarrow {}^4T_1g(P)$ $^4T_1g \rightarrow {}^4T_1g(F)$	4.87	Octahedral
$[Ni(L)(Q)(H_2O)_2]Cl$	70..1	227 286 360 640	44,05234,843 27,77715,625	2343 1878 1365 20	L.F L.F C.T $^3A_2g \rightarrow {}^3T_1g(P)$	4.61	Octahedral
$[Cu(L)(Q)]Cl\ .H_2O$	56.2	226 284 365 412 710	44,247 35,211 21,505 24,271 14,084	2278 1982 123432 27	L.F L.F C.T $^2B_1g \rightarrow {}^2Eg$ $B_1g \rightarrow {}^2A_2g$	1.78	Tetrahedral
$[Co(L)(PHH))(H_2O)_2Cl]Cl.$ H_2O	33.21	230 24٥ 357 396 762	43,478 40,816 28,089 25,252 13,123	1943 1582 582 325 38	L.F L.F C.T^6A_1g $\rightarrow {}^4A_1g(G),Eg(G)$ $^6A_1g \rightarrow {}^4T_2g(G)$	4.72	Octahedral
$[Ni(L)(PHH))(H_2O)_2Cl]Cl.$ H_2O	43.5	٢٢4 247 344 470	42,735 40,485 29,069 21,276	2143 1854 1342 45	L.F L.F C.T$^3A_2g \rightarrow {}^3T_1g(P)$	4.86	Octahedral
$[Cu(L)(PHH)\ (H_2O)_2Cl]Cl.$ H_2O	75.1	٢٢3 271 354 423 821	42,918 36,900 28,248 23,640 12,180	2278 1789 1345 827 32	L.F L.F C.T $^2Eg \rightarrow {}^2T_2g$	1.81	Octahedral

Thermal analysis

Thermal degradation of $[Co(L)(Q)(H_2O)_2]Cl.H_2O$ complex has been carried oututilizing (TGA) and TGA analysis[18]. The TGA-curve of $[Co(L)(Q)(H_2O)_2]Cl.H_2O$ complex appears, which the 1st step with 7.28% lack of the overall weight is attributed to the elimination of lack of Cl moiety and H_2O lattice between 50–120 °C. The 2nd step at 120–230 °C coincides with the lack of 2.45%, attributed to eliminating the H_2O chelated molecule. The 3rd step of degradation coincides with the lack of 23.19% at 250–300 °C attributed to the lack of L moiety. The final step at 300–460 °C, the lack of 28.25% of the overall weight, is attributed to the degradation of the complex and forming of CoO at <500 °C. The curve of TGA of the $[Cu(L)(PPH)(H_2O)_2Cl]Cl.H_2O$ complex appears a peek at 110 °C, coinciding with lattice rearrangement[19]. However, the mighty peak at 280–320 °C may be designated to degrade the anhydrous complex by lacking the organic molecule and forming CuO at <500 °C. The thermal degradation is indicated to conduct as next: The curve of TGA for$[Cu(L)(PPH)(H_2O)_2Cl]Cl.H_2O$appearsthreesteps[20].First, the absence of 10.12% of the complex's overall weight indicates the absence of $3H_2O$ crystalline molecules at 50–210 C. At 210–320 ºC, the second step corresponds to the absence of 13.35 % due to two Cl moieties. The final step coincides with the loss of 60.78% at 320–440 °C attributed to the complex degradation [14]. The remains were 15.75% of overall molecular weight attributed to the forming of CuO at <500 °C. The degradation at 440–500 °C emphasizes the fractional oxidation of the O^{-2}. Therefore, the curve of TGA of the hydrated coordinateappears2 peaks. The 1st peak at 145 °C is potentially attributed to lack of H_2O, but the 2nd peak at 330˚C coincides with the anhydrous complex's melting. Therefore, the degradation of the complex happens in the reign 440–500 °C [21].

Biological evaluation Antimicrobial activity

The metal chelates have been tested with diverse selected pathogens to evaluate their properties of biological. Bacteria included *Escherichia Coli*, *Bacillus subtilis, Eterobactern* and *Staphylococcus aureus.* In comparison, antifungal strains included *F.solani* and *C.cucurbitacin*.The ligands with 1,10-ph and 8-HQutilizing the well diffusion approach in the DMSO by nutrient agar at a (10^{-3}mole/L)were prepared through dissolving the complex. Due to depositing electrons on aromatic rings, residual complexes were more efficient (weakly/moderately) than predicted bonding in lowering metal atom polarity. This is growing the lipophilic character, favoring its penetration into membrane of the bacterial reason the death of living organisms [21].The outcomes are specified which the complexes were moderately efficient with all the fungi and bacteria .

The Cu(II)complexes, on the other hand, were very effective against the bacteria and fungi tested, with inhibitory area diameters ranging from 19.0 to 35.0 mm/mg. The increased Cu (II) and Ni (II) absorption through the cell wall/membrane may be the cause of this improved efficacy [22]. The Co(II) combination was also ineffective against bacterial and fungal strains with inhibitory zone widths of 13 to 23 mm/mg. Chelation is demonstrated by the ligands and complexes, improving biological efficacies. The following key elements must be considered while analyzing the complexes' biological effectiveness:

i) The coordinate influence of the ligands.

ii) The kind of N-granter ligands.

iii) The overall charge of complex.

iv) The kind and ion equalizing presence of ionic complex.

v) The nuclearity center of metal in the complex.

This is perhaps one of the causes for the complexes' various biological efficacy. At the same time, the metal ion-coordinating kind of ligand L may have an important role in this variety [23].

Table 4: Ligands and their metal complexes have antibacterial action

No.	Compound	*Staphylococcus aureus*	*Bacillus subtilis*	*Eterobactern*	*Escherichia Coli*	*Fusarium solani*	*Cercospora cucurbitacin*
1	[Co(L)(PHH)]Cl. H_2O	16	18	*20*	23	23	26
2	[Ni(L)(PPH)]Cl.H_2O	*28.0*	18	22	27	27	24
3	[Cu(L)(PPH)]Cl.H_2O	*19*	21	26	35	33	35
4	[Co(L)(Q)$(H_2O)_2$]Cl	13	17	20	23	28	30
5	[Ni(L)(PPH)$(H_2O)_2$]Cl	15	19	23	24	26	28
6	[Cu(L)(PPH)$(H_2O)_2$]Cl.H_2O	20	23	25	28	30	32
C	DMSO	_	_	_	_	-	-

Studies of DNA linking

UV-Vis spectroscopy has been used to carry out studies of DNA binding. Electronic absorption titration experiments were done at (pH 7.54) in 10 mMTris–HCl with extra amounts of (CT-DNA) with the complex concentration fixed at 2.50 x 10^{-4}M.[Cu(L)(PPH)$(H_2O)_2$]Cl compounds with and without CT-DNA absorption spectra. Both the complexes on adding CT-DNA appear a reduction in molar absorptivity (hypochromism of 64% for [Cu(L)(PPH)$(H_2O)_2$Cl] .H_2O and 87% or[Cu(L)(Q)$(H_2O)_2$Cl]Cl of the π → π* band suggesting powerful linking of the DNA to complexes[19].Intercalated complexes of stacked DNA base pairs and aromatic chromophore In order to compute quantitative rapprochement of the DNA linking capacity[24], we used Eq. (1).

$$\frac{[DNA]}{(\varepsilon_a - \varepsilon_f)} = \frac{[DNA]}{(\varepsilon_b - \varepsilon_f)} + \frac{1}{K_b(\varepsilon_b - \varepsilon_f)} \quad (1)$$

Where [DNA] is the CT-DNA concentration utilized, A plot of [DNA]/(εa − εf) against yields of [DNA] a slope = 1/(εb − εf), and the intercept = $1/K_b(\varepsilon_b - \varepsilon_f)$, εa, εf, and $_{\varepsilon b}$ coincide with coefficients of apparent extinction for complex, in other words, Abs/[complex] in the DNA existence, non-attendance, and bound DNA. The linking constant K_b has been estimated from the proportion of slope to intercept. K_b values are 1.89 x 10^5 M1 for [Cu(L)(PPH)$(H_2O)_2$Cl]Cl .$H_2O$and 3.76 x10^5 M1 for [Cu(L)(Q)$(H_2O)_2$Cl], respectively. Those outcomes were similar to those of a traditional intercalator. (pH 7.33) such as EB (K_b = 1.40 105 M1) in a Tris-HCl 25 mM buffer. The more hypochromism proportion (78.6%) and the more data of K_b for[Cu(L)(PPH)$(H_2O)_2$Cl]Cl .H_2Ocompared to Cu(L)(Q)$(H_2O)_2$Cl] suggests its more linking. The resulting slope is due to the 4 square chalets planar structure of [Cu(L)(PPH)$(H_2O)_2$Cl]Cl .H_2O [25].

Fluorescence spectral study for the competitive binding of the DNA

(EB.) is a highly helpful probe of DNA structure that exhales intensive fluorescence when linking to DNA in the range 600 nm through robustinter polation between neighboring base pairs of DNA. This fluorescence may be put out by adding various molecules which may substitute bound EB. Experiences of competitive linking were performed on CT-DNA bound to EB in 10 mM of Tris-HCl solution buffer by changing the complexes concentration in pH 7.9.It is displayed which in existence of all complexes, the intensity of fluorescence for DNA -bound EB reduced at 595nm as the compound concentrations grew [26]. This reduction in fluorescence intensity after adding complexes indicates that complexes compete with EB to link to DNA and substitute this separator, thus minimizing fluorescence intensity. The constants of quenching were determined utilizing the subsequent neutralization of Stern - Volmer:

$$\frac{F_0}{F} = 1 + K_{SV}[Q] \qquad (2)$$

Where K_{SV} is the constant of Stern–Volmer quenching and F and F_0represent emission intensity values of CT-DNA bound EB in existence and obscurity of quencher concentration of complex [Q], respectively. K_{SV} has been determined from slope of [complex] between F_0/Fplot. Data of Ksv were showntobe1.89 × 10^4, 2.05 × 10^4, 0.86 × 10^4, 3.55 × 10^4, 4.76 × 10^4, and 5.85 × 10^4 M^{-1} for the complexes.

The apparent linking constant K_{app} was determined utilizing the following equation:

$$K_{EB} \times [EB] = K_{app} \times [complex]_{50} \qquad (3)$$

Where [compound]50 is the concentration of compound quenching at 50% of the intensity of emission for the complexes bound of EB, the values for complexes were 14.67 x 105, 13.45 x 105, 12.98 x 105, 15.54 x 105, 16.65 x 105, and 17.50 x 105 M^{-1}.

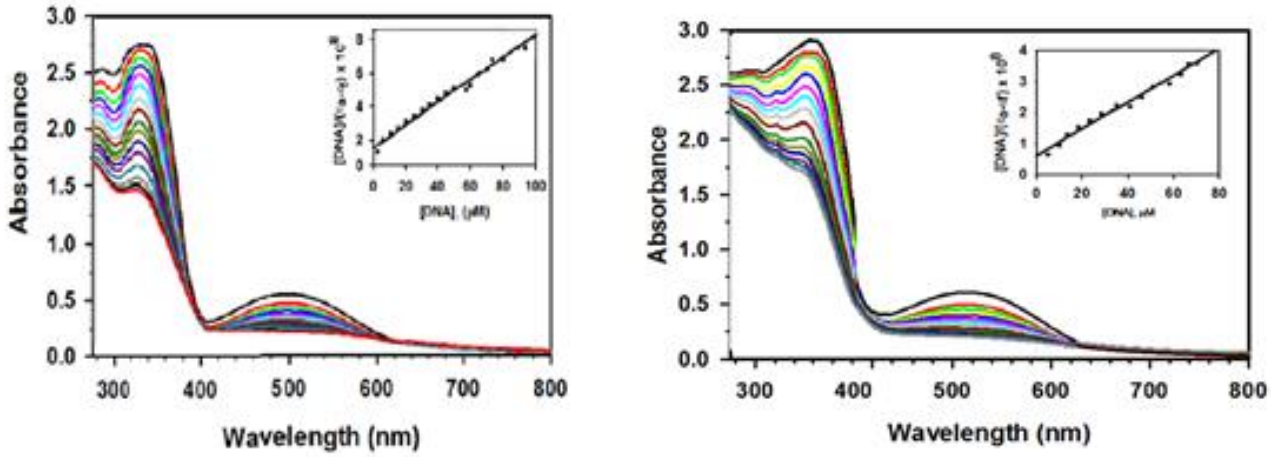

Figure 2: a) Titration with CT-DNA (0–90 M) diluted in 10mM Tris– HCl buffer results in a change in the electronic absorption spectra of 1 [2.5 10 4M] (pH 7.54). **b** After titrating with CT-DNA (0-85M) dissolved in 10mM Tris-HCl solution, the electronic absorption spectra of 2 [2.5 10 4M] changed (pH 7.54). **c** After titrating with CT-DNA (0-70M) dissolved in 10mM Tris-HCl solution, the electronic absorption spectra of 3 [2.5 10 4M] changed (pH 7.54). An increase in CT-DNA concentration causes the absorbance to drop, as indicated by the arrow. The graphic in the inset displays how [DNA]/(a f) vs [DNA] fits linearly.

Viscosity measurements

As a backing up guide to spectroscopic DNA insertion analyses displayed by all components, measurements of viscosity on CT-DNA by changing concentration of the appended compound wasled. Typically, it is noticed which η_{rel} for the solution of CT-DNA raises with substrates upon the interaction that links to intercalation. This is because inserting the between complex base pairs of DNA causes base pairs to split up, which raises the total DNA length, which leads to a rise in DNA viscosity. Adding augmentation amount of complexes on the η_{rel} showed a constant rise in the DNA viscosity that proposes intercalative method of DNA linking to Cu (II) complexes. Furthermore, it is to be observed which the increase in viscosity is more selected in the status of $[Cu(L)(Q)(H_2O)_2Cl]Cl$ [22].The outcomes backup spectroscopic studies indicating that compound$[Cu(L)(Q)(H_2O)_2Cl]Cl$ links higher mightily to CT-DNA [27].

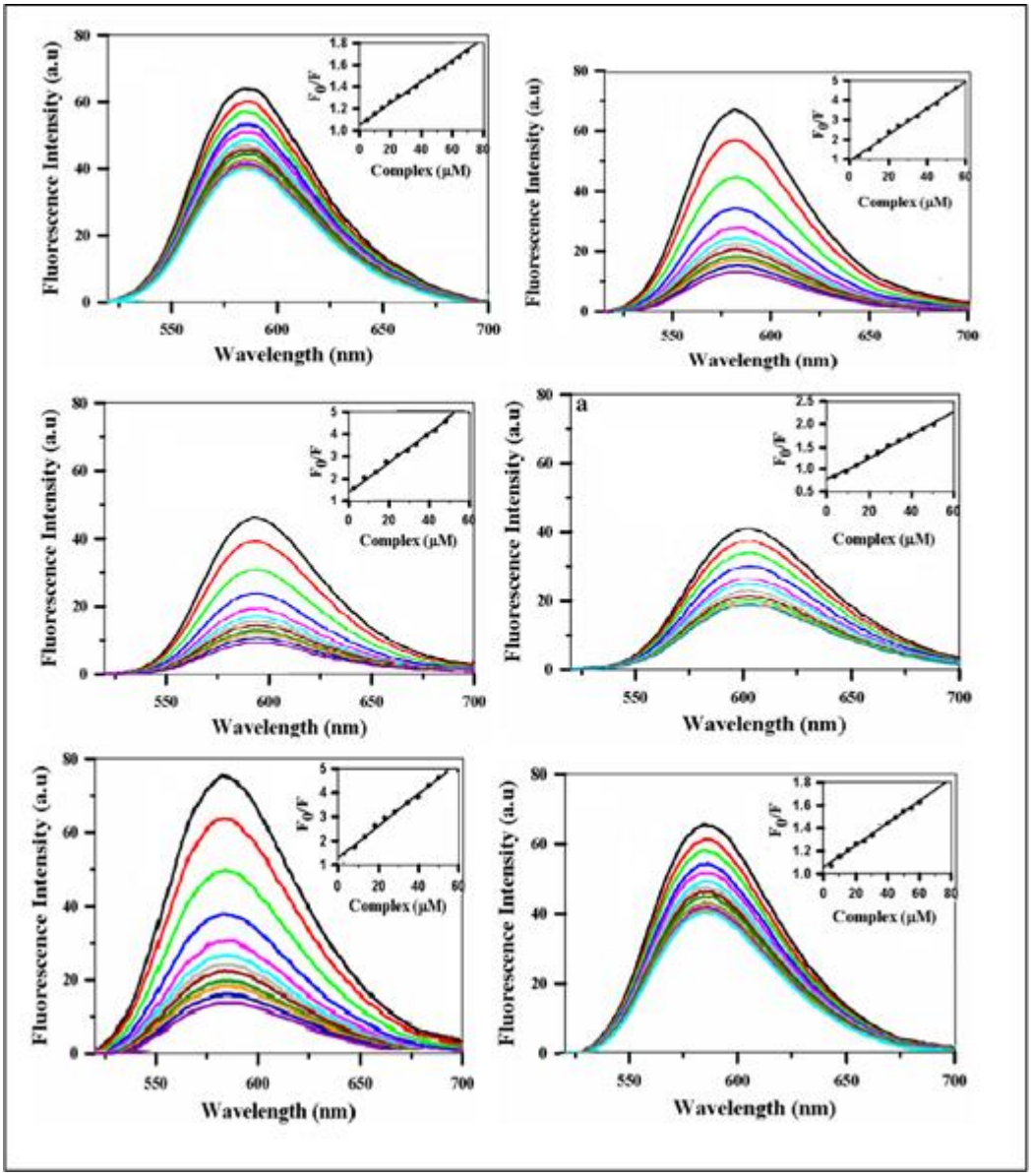

Figure 3: Spectra off luorescence emission of EB (2 μM) bound to(50 μM) CT-DNA in non-attendance and the existence of Cu (II) complexes: in (pH 7.9)10 mM buffer of Tris–HCl, λex = 510 nm at different concentrations

Cytotoxicity

Here we examine the effects of synthesized L ligand and its mixed-metal complexes with 1,10-phenanthroline/hydroxyquinoline on the viability of L132, MCF-7, and HaCaT cell lines in vitro.A549 lung cancer cells were treated for 48 hours with various complex doses of mitochondrial hydrogenaseenzyme. As shown by their 70% and 84% viability, [Co(L)(PPH)Cl] complexes were shown to be hazardous to MCF-7 cells at 2M concentration. In comparison, at the same dose, the toxicity is proportionally lower in cells HaCaT (survival Cell 90% for $[Cu(L)(PPH)(H_2O)_2Cl]Cl.H_2O$ and 95% for$[Cu(L)(Q)(H_2O)_2Cl]$ Practically no toxicity appeared to L132 lung cells treated with twoμM M of [Ni(L)(PPH)Cl] and$[Ni(L)(Q)(H_2O)_2Cl]$.This is compared to the same dose viability of 89 percent and 86 percent in L132 cells treated with [Ni(L)(PPH)Cl] and$[Ni(L)(Q)(H_2O)_2]Cl$.Moreover,at5μM dose of$[Cu(L)(PPH)(H_2O)_2Cl]Cl.H_2O$ appears comparable outcomes in HaCaTcells as suggested by 91% cell viability. A similar observation was found in the case wheretheA549 cells have been treated with 10 μM dosage of [Ni(L)(PPH)Cl] and$[Ni(L)(Q)(H_2O)_2]Cl$, cell viability was decreased to 30% and 40% for [Ni(L)(PPH)Cl]

and[Ni(L)(Q)$(H_2O)_2$]Cl. At the same time, the complexes seem be much less toxic to L132 cells displaying viability of 80% and 73%, respectively, on therapy with μM dosage of [Cu(L)(PPH)$(H_2O)_2$Cl]Cl .H_2O and[Cu(L)(8Q)$(H_2O)_2$Cl**]**. When HaCaT cells are treated with a one M dose of [Ni(L)(PPH)Cl] and [Ni(L)(8Q)$(H_2O)_2$Cl], viability appears to be thoroughly modest (50 %).Again, a considerable variation in viability was noticed when likening the influence of the 2,5 and 10 Mm dose of[Cu(L)(PPH)Cl] and[Cu(L)(Q)$(H_2O)_2$Cl]Cl on the A549 cells versus L132 cells. For the whole concentration range studied, [Co(L)(PPH)Cl] was shown to be more harmful than [Co(L)(Q)$(H_2O)_2$Cl], but considerably less toxic when compared to A549 cells in the MCF7 cell line. Cu(L)(PPH)Cl and Cu(L)(Q)$H_2O)_2$Cl]Cl are both toxic to HaCaT cells at doses of 2M and higher. However, at 10M, [Co(L)(Q)$(H_2O)_2$]Cl is found to be significantly less toxic than [Co(L)(PPH)Cl], as evidenced by their cell viabilities of 30% and 25%, respectively.

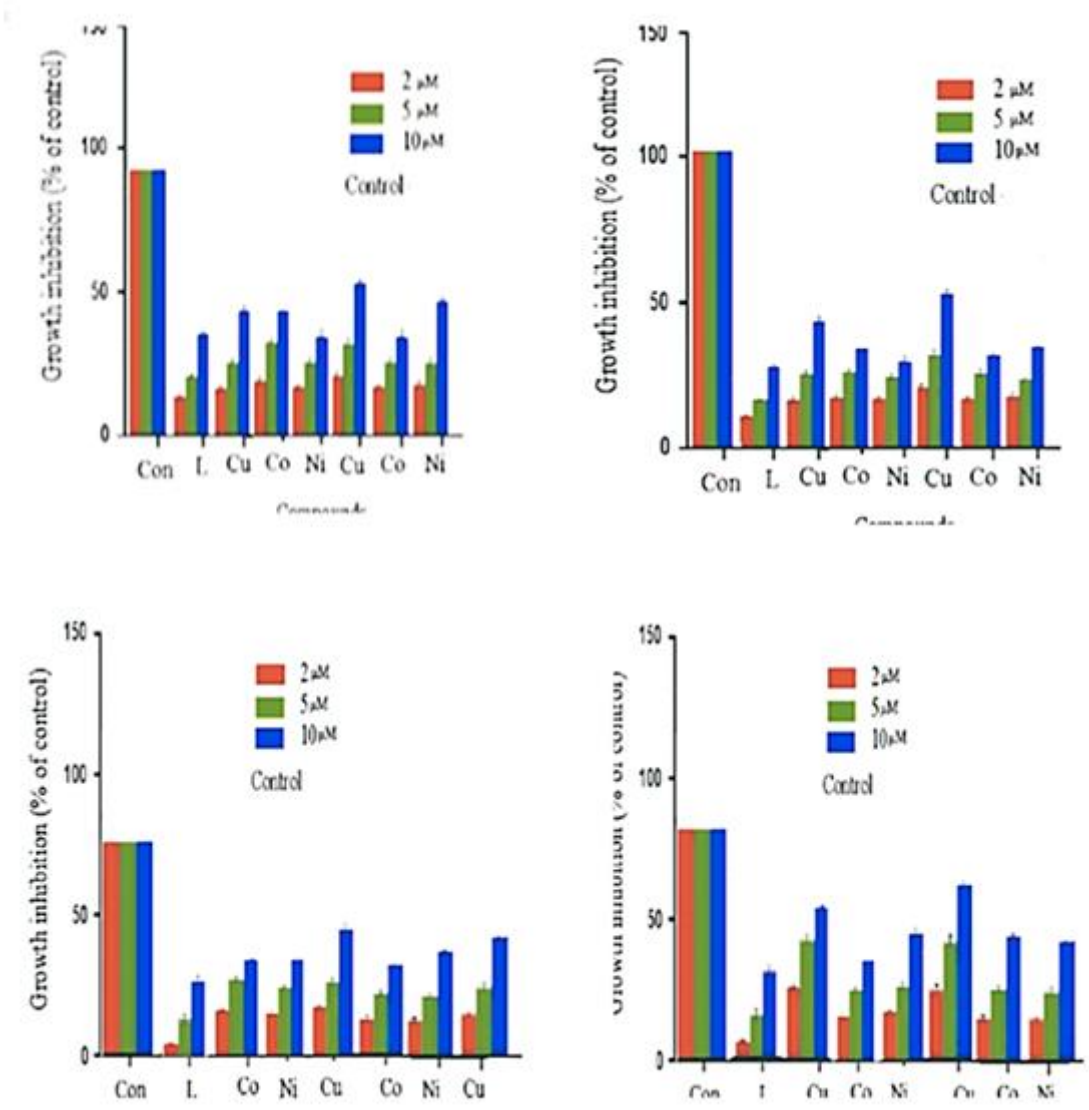

Figure 4: (a) Concentration-based growth inhibition (HaCaT), (b) Concentration-based growth inhibition (L132), (c) Concentration-based growth inhibition (MCF-7) and (d) growth inhibition dependent on concentration (A549)

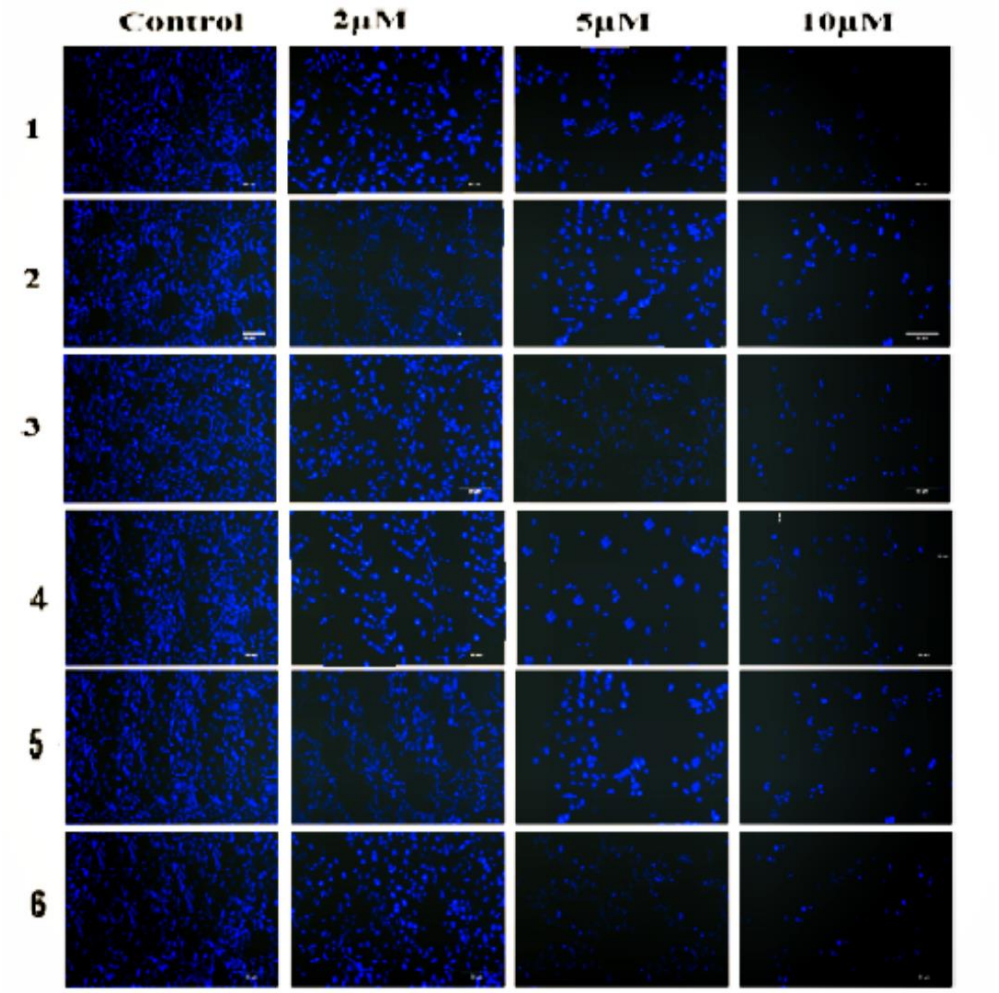

Figure 5: luorescence microscopic photos demonstrating the impact of 1-3 incremental dosages on DAPI-stained HeLa cells

Conclusion

Six novel mixed-ligand complexes of Ni(II), Co(II), and Cu(II) based on Schiff base that had been derived from benzophenone with trimethoprim as a primary ligand and (1,10-Phen) and (8-HQ) as a 2nd-ligandmay be artificially defied to fine-tune the metal complexes features and have been appeared to show. The six coordinated metal-ligand complexes in the produced complexes can have an octahedral shape. They were composed and described by diverse physicochemical methods such as magnetic moment, IR, electronic, NMR, and thermal. Co(II), Ni(II), and Cu(II) complexes created during synthesis of the Schiff base have octahedral structure (for 1,10-Phen). Cu (II) complexes have square planar shape, on the other hand (for 8-HQ).Mixed ligand complexes with antifungal and antibacterial properties have been tested against the pathogenic strains strains of bacteria and fungus types, which are *Escherichia Coli*, *Bacillus subtilis, Eterobactern* and *Staphylococcus aureus, F.solani and C.cucurbitacin*. MCF-7, HaCaT, and A549 anticancer cell lines were studied. The outstanding result of mixed Cu(II) complexes was highlighted.

Acknowledgments

The authors are thankful to the Chairman, Department of Chemistry, *College of Education for Pure Science, Ibn Al-Haitham, University of Baghdad, Iraq*

Funding

This research did not receive any specific grant from funding agencies in the public, commercial, or not-for-profit sectors.

Authors' contributions

All authors contributed toward data analysis, drafting and revising the paper and agreed to responsible for all the aspects of this work.

Conflict of Interest

Authors have declared that they have no known competing financial interests or non-financial

ORCID:

Hiyam Hadi Alkam
https://orcid.org/0000-0002-1750-0576
Rehab K. Al-Shemary
https://orcid.org/0000-0002-6761-7131

References

[1]. Demirezen N., Tarınç D., Polat D., Çeşme M., Gölcü A., Tümer M., Synthesis of trimethoprim metal complexes: Spectral, electrochemical, thermal, DNA-binding and surface morphology studies. *Spectrochimica Acta Part A: Molecular and Biomolecular Spectroscopy*, 2012, **94**:243-255 [Crossref], [Google Scholar], [Publisher]

[2]. Sumalatha V., Rambabu A., Vamsikrishna N., Ganji N., Daravath S., Synthesis, characterization, DNA binding propensity, nuclease efficacy, antioxidant and antimicrobial activities of Cu (II), Co (II) and Ni (II) complexes derived from 4-(trifluoromethoxy) aniline Schiff bases. *Chemical Data Collections*, 2019, **20**:100213 [Crossref], [Google Scholar], [Publisher]

[3]. Gülcan M., Sönmez M., Berber İ., Synthesis, characterization, and antimicrobial activity of a new pyrimidine Schiff base and its Cu (II), Ni (II), Co (II), Pt (II), and Pd (II) complexes. *Turkish Journal of Chemistry*, 2012, **36**:189 [Crossref], [Google Scholar], [Publisher]

[4]. Alaghaz A.M.A., Farag R.S., Elnawawy M.A., Ekaw A.D.A., Synthesis and spectral characterization studies of new trimethoprim-diphenylphosphate metal complexes. *International Journal of Science and Research,* 2016, **5**:1220 [Crossref], [Google Scholar], [Publisher]

[5]. Cebotaru L., Liu Q., Yanda M.K., Boinot C., Outeda P., Huso D.L., Watnick T., Guggino W.B., Cebotaru V., Inhibition of histone deacetylase 6 activity reduces cyst growth in polycystic kidney disease. *Kidney international*, 2016, **90**:90 [Crossref], [Google Scholar], [Publisher]

[6]. Saif M., El-Shafiy H.F., Mashaly M.M., Eid M.F., Nabeel A.I., Fouad R., Synthesis, characterization, and antioxidant/cytotoxic activity of new chromone Schiff base nano-complexes of Zn (II), Cu (II), Ni (II) and Co (II). *Journal of Molecular Structure*, 2016, **1118**:75 [Crossref], [Google Scholar], [Publisher]

[7]. Al-Shemary R.K., Sultan J.S., Lateef S.M., Synthesis and Characterization of Some New Complexes with New Schiff Base Type (N_2O_2) Derived From Glyoxylic Acid and Ethylenediamine. *Ibn AL-Haitham Journal For Pure and Applied Science*, 2017, **28** [Google Scholar]

[8]. Kosak U., Brus B., Knez D., Zakelj S., Trontelj J., Pislar A., Sink R., Jukic M., Zivin M., Podkowa A., Nachon F., The magic of crystal structure-based inhibitor optimization: development of a butyrylcholinesterase inhibitor with picomolar affinity and in vivo activity. *Journal of Medicinal Chemistry*, 2018, **61**:119 [Crossref], [Google Scholar], [Publisher]

[9]. Natiq Ahmed N. G., Al-Hashimi H. Y., Preparation and characterization of some new Schiff bases compounds with the study of biological effectiveness. *International journal of current research in biosciences and plant biology,* 2016, **3**:127 [Crossref], [Publisher]

[10]. Al-Shemary R.K.R., Microwave Preparation, Spectral Studies and Antimicrobial Activities Evaluation of Mn (II), Ni (II), Hg (II), Co (II) and Cu (II) Complexes with Schiff Base Ligand. *Ibn AL-Haitham Journal for Pure and Applied Sciences*, 2017, **30**:58 [Crossref], [Google Scholar], [Publisher]

[11]. Krátký M., Dzurková M., Janoušek J., Konečná K., Trejtnar F., Stolaříková J., Vinšová J., Sulfadiazine salicylaldehyde-based Schiff bases: Synthesis, antimicrobial activity and cytotoxicity. *Molecules*, 2017, **22**:1573 [Crossref], [Google Scholar], [Publisher]

[12]. Abdul A.P.D.L.K., Jaafar K.L.D.W.A., Synthesis, Characterization and Biological Activity of Schiff Bases Chelates with Mn (II), Co (II), Ni (II), Cu (II) and Hg (II). *Baghdad Science Journal*, 2017, **14**:2 [Google Scholar], [Publisher]

[13]. Zaidan B.A.H., Majeed N.M., Al-Shemary R.K., Numan A.T., Synthesis of some Schiff base metal complexes involving trimethoprim and 2'-amino-4-chlorobenzophenone: Spectral, thermal, DNA Cleavage antimicrobial, antifungal and Cytotoxic activity studies. *Journal of Pharmaceutical Sciences and Research*, 2019, **11**:618 [Google Scholar], [Publisher]

[14]. Adam R.W., Al-Labban H.M.Y., Aljanaby A.A.J., Abbas N.A., Synthesis, Characterization and Antibacterial Activity of Some Novel 1, 2, 3-Triazol-Chalcone Derivatives from N-Acetyl-5H-Dibenzo [b, f] Azepine-5-Carboxamide. *Nano Biomedicine and Engineering,* 2019, **11**:99 [Google Scholar], [PDF]

[15]. Beale J.M., Block J., Hill R., *Organic medicinal and pharmaceutical chemistry*. Philadelphia: Lippincott Williams & Wilkins. 2010 [Google Scholar], [PDF]

[16]. Venkateswarlu K., Ganji N., Daravath S., Kanneboina K., Rangan K., Crystal structure, DNA interactions, antioxidant and antitumor activity of thermally stable Cu (II), Ni (II) and Co (III) complexes of an N, O donor Schiff base ligand. *Polyhedron*, 2019, **171**:86 [Crossref], [Google Scholar], [Publisher]

[17]. Bahamondes C., Wilson L., Aguirre C., Illanes A., Comparative study of the enzymatic synthesis of cephalexin at high substrate concentration in aqueous and organic media using statistical model. *Biotechnology and Bioprocess Engineering,* 2012, **17**:711 [Crossref], [Google Scholar], [Publisher]

[18]. Al Zoubi W., Biological activities of Schiff bases and their complexes: a review of recent works. *International Journal of Organic Chemistry*, 2013, **2013** [Crossref], [Google Scholar], [Publisher]

[19]. Tomi I.H.R., Abdullah A.H., Al-Daraji A.H.R., Abbass S.A.R., Synthesis, characterization and comparative study the antibacterial activities of some imine-amoxicillin derivatives. *European Journal of Chemistry*, 2013, **4**:153 [Crossref], [Google Scholar], [Publisher]

[20]. Waziri I., Ndahi N.P., Mala G.A., Fugu M.B., Synthesis, spectroscopic and biological studies of Cobalt (II), Nickel (II) and Iron (III) mixed antibiotic metal complexes. *Der Pharma Chemica,* 2014, **6**:118 [Google Scholar], [PDF]

[21]. Koyuncu I., Gonel A., Kocyigit A., Temiz E., Durgun M., Supuran C.T., Selective inhibition of carbonic anhydrase-IX by sulphonamide derivatives induces pH and reactive oxygen species-mediated apoptosis in cervical cancer HeLa cells. *Journal of Enzyme Inhibition and Medicinal Chemistry*, 2018, **33**:1137 [Crossref], [Google Scholar], [Publisher]

[22]. Okolotowicz K.J., Dwyer M., Ryan D., Cheng J., Cashman E.A., Moore S., Mercola M., Cashman J.R., Novel tertiary sulfonamides as potent anti-cancer agents. *Bioorganic & Medicinal Chemistry*, 2018, **26**:4441 [Crossref], [Google Scholar], [Publisher]

[23]. Bonakdar A.P.S., Vafaei F., Farokhpour M., Esfahani M.H.N., Massah A.R., Synthesis and anticancer activity assay of novel chalcone-sulfonamide derivatives. *Iranian Journal of Pharmaceutical Research: IJPR*, 2017, **16**:565 [Google Scholar], [Publisher]

[24]. Reddy N.D., Shoja M.H., Biswas S., Nayak P.G., Kumar N., Rao C.M., An appraisal of cinnamyl sulfonamide hydroxamate derivatives (HDAC inhibitors) for anti-cancer, anti-angiogenic and anti-metastatic activities in human cancer cells. *Chemico-biological interactions*, 2016, **253**:112 [Crossref], [Google Scholar], [Publisher]

[25]. Sławiński J., Szafrański K., Vullo D., Supuran C.T., Carbonic anhydrase inhibitors. Synthesis of heterocyclic 4-substituted pyridine-3-sulfonamide derivatives and their inhibition of the human cytosolic isozymes I and II and transmembrane tumor-associated isozymes IX and XII. *European Journal of Medicinal Chemistry*, 2013, **69**:701 [Crossref], [Google Scholar], [Publisher]

[26]. Mohammed A., Al Shemary R.K.R., Metal complexes with heteroscorpionate ligand founded

on the pyridinamine group: cyclin-dependent kinase 2 inhibitor antimicrobial, antioxidant, and in vitro cytotoxicity, notional studies. *International Journal of Pharmaceutical Research*, 2021, **13** [Crossref], [Google Scholar], [Publisher]

[27]. Majeed N.M., Abd S.S., Al Shemary R.K.R., Eco-friendly and Efficient Composition, Diagnosis, Theoretical, kinetic studies, Antibacterial and Anticancer Activities of Mixed Some Metal Complexes of Tridentate Schiff base Ligand. *International Journal of Pharmaceutical Research*, 2021, **13** [Google Scholar]

HOW TO CITE THIS ARTICLE
Hiyam Hadi Alkam, Rehab K. Al-Shemary. Microwave Synthesis Schiff Base from Drug and 1,10-Phenanthroline/8-Hydroxyquinoline as a Co-ligand with Complexes: Cytotoxic, Antimicrobial, and DNA Interaction Efficacy, *J. Med. Chem. Sci.*, 2022, 5(7) 1331-1346
https://doi.org/10.26655/JMCHEMSCI.2022.7.22
URL: http://www.jmchemsci.com/article_155658.html